Electronic Supplementary Material (ESI) for Environmental Science: Processes & Impacts.

Supplementary Information for

Diel Mercury Concentration Variations in a Mercury-Impacted Stream

Scott C. Brooks*, Ami L. Riscassi, Carrie L. Miller, Kenneth A. Lowe,
Xiangping Yin, Tonia L. Mehlhorn

1. ESTIMATES OF CHANNEL CANOPY COVER

To estimate the difference in creek channel canopy cover in summer versus winter, we used GoogleEarth Pro (version 7.3.4.8573) to compare aerial photographs taken in February 2021 to those taken in June 2021 (EFK 5.4 and EFK 16.2) or June 2019 (EFK 23.4, the channel was obscured by clouds in the June 2021 photograph, no photograph available for June 2020). The area of water surface visible in these photographs was estimated using the polygon feature in GoogleEarth beginning from our sampling location and extending a distance upstream equal to 15 channel widths. The area circumscribed by the polygons was summed and used to estimate the extent of canopy cover in summer versus winter. This likely underestimates canopy cover at EFK 5.4 for the sampling campaigns in this paper as we know of several trees that fell between August 2018 and February 2021. Aerial photographs closer in time to our sampling campaigns were of poorer quality or did not have contrasting leaf on – leaf off images available.

2. DISCHARGE MEASUREMENTS

Stream stage at EFK 5.4 and EFK 16.2 was measured and recorded at 15-minute intervals by a pressure transducer within a stilling well at each site. Stream stage (meters) was converted to discharge (cubic meters per second, $m^3 \cdot s^{-1}$) using stage-discharge relationships developed for each site. Discharge data at 6-minute intervals for EFK 23.4 were provided by Y-12 NSC Environmental Compliance. Daily mean discharge data for the ORWTF was provided by the City of Oak Ridge, TN (Table S.4).

3. QUALITY ASSURANCE/QUALITY CONTROL

Instrument performance for both Hg and MMHg samples was verified with standards throughout the analytical run, matrix spikes, analytical duplicates (distillation duplicates for MMHg) and system blanks. For MMHg analysis, distillation blanks were also run to verify no contamination was introduced in that process. Field duplicates and field blanks were also collected. Detection limits for Hg and MeHg were determined for each analytical run based on methods outlined in Oppenheimer et al. [1]; for Hg analysis, minimum detection ranged from 0.15 to 0.59 $ng \cdot L^{-1}$ (mean 0.37 ± 14 $ng \cdot L^{-1}$) based on analysis of 20 mL of sample and for MMHg, 0.011 to 0.025 $ng \cdot L^{-1}$ (mean of 0.015 ± 0.005 $ng \cdot L^{-1}$) based on analysis of a 45 mL sample. All samples analyzed were above the detection limit.

For Hg, mean recovery for matrix spikes was 101.2 ± 12.1%, and the mean relative percent difference (RPD) between analytical duplicates was 2.7 ± 1.5 %. The mean RPD for field duplicates for Hg_D and Hg_T were 7.3 ± 7.8% and 5.0 ± 5.6%, respectively. All field blanks were below detection limits for Hg. For MMHg, mean recovery for matrix spikes was 99.77 ± 4.25 %. The mean RPD between MMHg distillation duplicates was 8.3 ± 9.7 %. The RPD between field duplicates of filtered and total MMHg was 5.6 ± 5.0% and 7.4 ± 6.9%, respectively. Field blanks and distillation blanks for MMHg were below detection limits.

The mean RPD of field duplicates for all parameters is given in Table S.3.

4. SOLID-WATER PARTITIONING COEFFICIENTS

Solid-water partitioning coefficients (K_{SW}) were calculated for Hg and MMHg as (using Hg as an example):

$$K_{SW} = \frac{\frac{Hg_T - Hg_D}{TSS}}{Hg_D} \tag{1}$$

Where K_{SW} = solid-water partitioning coefficient ($L \cdot kg^{-1}$), Hg_T = total Hg ($ng \cdot L^{-1}$), Hg_D = dissolved Hg ($ng \cdot L^{-1}$), and TSS = total suspended solids ($kg \cdot L^{-1}$). The K_{SW} calculation is identical to that for the equilibrium distribution coefficient (K_D) used to describe linear equilibrium sorption isotherms. Here we adopt a more conservative interpretation and do not consider K_{SW} equal to the K_D because conditions did not conform to equilibrium sorption isotherm interpretation. Specifically, (i) the pH and temperature of the creek water varied within and between sampling events, (ii) the equilibrium condition is uncertain (i.e., cannot rule out kinetic effects), (iii) partitioning behavior may be under the control of processes other than reversible sorption (e.g., precipitation-dissolution reactions).

5. OUTLIER DETECTION

Because of the small number of samples at each site within a sampling campaign, potential outliers were determined using modified z-scores [2] due to the recognized limitations of the standard z-score for small sample size [3]. The modified z-score is calculated:

$$z_i = 0.6745\left(\frac{x_i - \tilde{x}}{MAD}\right) \tag{2}$$

Where z_i = modified z-score for observation *i*; x_i = observation *i*; $\tilde{x}$ = median for all observations; MAD = median absolute deviation of observations $= median(|x_i - \tilde{x}|)$. Observations with an absolute value z-score greater than 3.5 were flagged as possible outliers.

6. DETECTION OF NON-MONOTONIC ASSOCIATION

Chatterjee [4] introduced a new correlation coefficient (ξ) to enable detection of non-monotonic associations including oscillatory behavior of the type in which we were interested. Calculated values of ξ depend on the number of observations and the noise level in the data – see Figure S.1 – and appears to be fairly robust. Additionally, the measure is a function of ranks making it resistant to outliers. An important difference between ξ and other measures of correlation is that ξ is direction agnostic, i.e., while ξ can take on negative values it does not imply negative correlation. Rather, it indicates lack of correlation between the variables.

Table S.1. Coordinates (decimal degrees) for sampling sites and meteorological tower

Site	Latitude	Longitude
EFK 5.4	35.966287	-84.358178
ORWTF outfall	35.990574	-84.317544
EFK 16.2	35.998857	-84.300050
EFK 23.4	35.996375	-84.240020
Meteorological tower (Tower K)	35.933336	-84.386511

Table S.2. Water quality parameters measured during each diel sampling campaign

Parameter	Units	Su2013	Monthly AM/PM	W2014	Su2015	Su2018
	Event	Su2013	Monthly AM/PM	W2014	Su2015	Su2018
	Site	EFK 5.4	EFK 5.4	EFK 5.4	EFK 5.4, EFK 16.2, EFK 23.4	EFK 5.4
Field Measurements[a]						
discharge	$m^3 \cdot s^{-1}$	×	×	×	×	×
DO[b]	$mg \cdot L^{-1}$	×	×	×	×	×
FDOM[c]	ppb QSE	×	×			
Illuminance[d]	Lux				×	
PAR[e]	$\mu mole \cdot m^{-2} \cdot s^{-1}$	×		×		
pH	SU	×	×	×	×	×
SpecCond	$\mu S \cdot cm^{-1}$	×	×	×	×	×
Temperature	°C	×	×	×	×	×
Turbidity	NTU	×[e]		×[f]	×[g]	
Laboratory Analyses						
A.254	AU	×		×	×	
aluminum	$\mu g \cdot L^{-1}$	×		×	×	
ammonium	$\mu g\text{-}N \cdot L^{-1}$	×		×	×	
barium	$\mu g \cdot L^{-1}$	×		×	×	
bromide	$mg \cdot L^{-1}$				×	
calcium	$mg \cdot L^{-1}$	×		×	×	
chloride	$mg \cdot L^{-1}$	×		×	×	
DGM[h]	$ng \cdot L^{-1}$	×		×		
DIC[i]	$mg \cdot L^{-1}$	×		×		
DOC[j]	$mg \cdot L^{-1}$	×		×	×	
Hg_P:TSS[k]	$mg \cdot kg^{-1}$	×	×	×	×	
Hg_D[l]	$ng \cdot L^{-1}$	×	×	×	×	×
Hg_D:DOC[m]	$ng \cdot mg^{-1}$	×		×	×	
Hg_P[n]	$ng \cdot L^{-1}$	×	×	×	×	×
Hg_T[o]	$ng \cdot L^{-1}$	×	×	×	×	×
iron	$\mu g \cdot L^{-1}$	×		×	×	
$logK_{sw,Hg}$[p]	$L \cdot kg^{-1}$	×		×	×	
$logK_{sw,MMHg}$[p]	$L \cdot kg^{-1}$	×		×	×	
magnesium	$mg \cdot L^{-1}$	×		×	×	
manganese	$\mu g \cdot L^{-1}$	×		×	×	
$MMHg_P$:TSS[q]	$mg \cdot kg^{-1}$	×	×	×	×	
$MMHg_D$[r]	$ng \cdot L^{-1}$	×	×	×	×	×
$MMHg_D$:DOC[s]	$ng \cdot mg^{-1}$	×		×	×	
$MMHg_P$[t]	$ng \cdot L^{-1}$	×	×	×	×	×
$MMHg_T$[u]	$ng \cdot L^{-1}$	×	×	×	×	×
nitrate	$mg \cdot L^{-1}$	×		×	×	
Pct.C[v]	%	×		×		
phosphate	$mg \cdot L^{-1}$				×	
POC[w]	$mg \cdot L^{-1}$	×		×		
potassium	$mg \cdot L^{-1}$	×		×	×	
SlopeRatio	dimensionless	×		×	×	
sodium	$mg \cdot L^{-1}$	×		×	×	
SRP[x]	$\mu g\text{-}P \cdot L^{-1}$	×		×	×	
strontium	$\mu g \cdot L^{-1}$	×		×	×	
sulfate	$mg \cdot L^{-1}$	×		×	×	
SUVA.254	$L \cdot mg\text{-}C^{-1} \cdot m^{-1}$	×		×	×	
TSS[y]	$mg \cdot L^{-1}$	×	×	×	×	
uranium	$\mu g \cdot L^{-1}$	×		×	×	

[a] unless indicated otherwise, these parameters were measured and recorded with a YSI 600 multiparameter sonde. For the Su2015 campaign, a YSI 6920 v2 sonde was used at EFK 16.2 and an In Situ Troll 9000 Pro was used at EFK 23.4

[b] dissolved oxygen

[c] fluorescent dissolved organic matter measured in units of parts per billion quinine sulfate equivalent; measured and recorded using a Turner C6 multi sensor sonde

[d] measured with HOBO Pendant® light meter which measured and recorded light intensity over the wavelength range 150 – 1200 nm

[e] photosynthetically active radiation, measured with a Li-Cor Quantum sensor and recorded on a Li-Cor LI-1000 data logger

[f] For Su2013 and W2014 turbidity was measured and recorded using a Turner C6 multi sensor sonde
[g] turbidity was not measured at EFK 23.4
[h] DGM = dissolved gaseous mercury
[i] dissolved inorganic carbon
[j] nonpurgeable dissolved organic carbon
[k] ratio of Hg_P to TSS
[l] dissolved total Hg
[m] ratio of Hg_D to DOC
[n] particulate Hg. Calculated as difference between Hg_T and Hg_D
[o] total Hg
[p] log_{10} of the solid:water partitioning coefficient for Hg or MMHg
[q] ratio of $MMHg_P$ to TSS
[r] dissolved MMHg
[s] ratio of $MMHg_D$ to DOC
[t] particulate MMHg. Calculated as difference between $MMHg_T$ and $MMHg_D$
[u] total MMHg
[v] percent carbon content of suspended solids
[w] particulate organic carbon
[x] soluble reactive phosphorous
[y] total suspended solids

Table S.3. Mean and standard deviation of the relative percent difference (RPD) for field duplicates, excluding values that were below detection

Parameter	Mean_RPD	StDev_RPD	n
A_{254}	2.5	2.1	21
aluminum	39.9	41.8	19
ammonium.N	18.9	23.9	15
barium	9.9	16.2	21
bromide	4.3	3.1	4
calcium	0.8	0.9	19
chloride	1.0	2.2	21
DGM	11.9	9.1	3
DOC	4.4	4.2	20
Hg_D	7.3	7.8	25
Hg_T	5.0	5.6	23
iron	20.9	42.1	18
magnesium	1.2	1.3	21
manganese	16.1	32.4	18
$MMHg_D$	5.6	5.0	24
$MMHg_T$	7.4	6.9	23
nitrate	1.6	2.8	21
phosphate	6.8	9.6	6
POC	15.3	11.0	12
potassium	1.5	1.6	21
SlopeRatio	4.5	5.5	21
sodium	1.4	1.5	21
SRP.P	7.6	7.8	21
strontium	1.1	0.8	21
sulfate	1.0	2.0	21
$SUVA_{254}$	5.6	4.9	21
TSS	10.3	8.6	21
uranium	1.3	1.4	21

Table S.4. Mean daily discharge ($m^3 \cdot s^{-1}$) summary during each sampling campaign (Figure S.3)

	Su2013			W2014			Su2015			
Site	EFK 5.4	ORWTF	EFK 23.4	EFK 5.4	ORWTF	EFK 23.4	EFK 5.4	ORWTF	EFK 16.2	EFK 23.4
	1.1	0.14	0.28	1.7	0.18	0.30	0.73	0.11	0.42	0.095

Table S.5. Dependence of parameter value on sampling time (ξ). sd = standard deviation of ξ; pval = adjusted p-value [5]. Entries in bold typeface have pval ≤ 0.05. Entries in bold red typeface have pval ≤ 0.05 and display non-monotonic oscillations. bdl = most results below method reporting limits. Blanks = parameter not measured

Campaign	Su2013			W2014			Su2015								
Site	EFK 5.4			EFK 5.4			EFK 5.4			EFK 16.2			EFK 23.4		
Variable	ξ	sd	pval	ξ	sd	pval	ξ	sd	pval	ξ	sd	pval	ξ	sd	pval
A.254	**0.4830**	0.1324	4.54E-04	**0.5227**	0.1324	1.44E-04	**0.4417**	0.1460	5.52E-03	**0.7957**	0.1501	2.31E-06	**0.4063**	0.1546	1.43E-02
aluminum	-0.0849	0.1319	7.59E-01	-0.1045	0.1323	7.85E-01	0.2167	0.1460	1.02E-01	0.0265	0.1513	4.30E-01	-0.1771	0.1546	8.74E-01
ammonium.N	0.1193	0.1324	2.09E-01				0.0500	0.1460	4.07E-01	0.0526	0.1501	3.92E-01	0.2396	0.1546	1.10E-01
barium	0.1943	0.1372	1.04E-01	0.0153	0.1340	5.20E-01	0.1667	0.1460	1.81E-01	0.2130	0.1512	1.10E-01	-0.0729	0.1546	6.99E-01
calcium	**0.4936**	0.1522	1.87E-03	**0.3310**	0.1334	1.24E-02	0.1425	0.1542	2.45E-01	**0.5307**	0.1518	5.55E-04	**0.5476**	0.1553	1.88E-03
chloride	**0.6420**	0.1324	7.35E-06	**0.6705**	0.1324	2.07E-06	**0.5583**	0.1460	6.56E-04	**0.6563**	0.1501	6.14E-05	**0.3438**	0.1546	3.27E-02
DOC	**0.2688**	0.1350	3.53E-02	**0.3239**	0.1328	1.32E-02	**0.4240**	0.1461	6.64E-03	**0.4985**	0.1501	8.98E-04	**0.5782**	0.1538	1.83E-03
Hg_{D}	**0.3352**	0.1324	1.11E-02	**0.4773**	0.1324	4.48E-04	-0.0250	0.1460	5.83E-01	**0.5728**	0.1501	3.02E-04	**0.5313**	0.1546	1.96E-03
Hg_{D}:DOC	-0.0114	0.1324	5.62E-01	**0.4489**	0.1324	8.24E-04	0.0083	0.1460	5.02E-01	**0.5356**	0.1501	4.79E-04	0.1563	0.1546	2.15E-01
$Hg_{P.ngL}$	**0.4034**	0.1324	2.90E-03	**0.3011**	0.1324	1.84E-02	**0.2917**	0.1460	3.88E-02	**0.5356**	0.1501	4.79E-04	-0.0417	0.1546	6.55E-01
Hg_{P}:TSS	**0.4148**	0.1324	2.54E-03	-0.0966	0.1324	7.85E-01	**0.3083**	0.1460	3.31E-02	**0.3777**	0.1501	1.08E-02	0.0521	0.1546	4.33E-01
Hg_{T}	**0.3750**	0.1324	4.75E-03	**0.3068**	0.1324	1.71E-02	**0.2833**	0.1460	4.18E-02	**0.5356**	0.1501	4.79E-04	0.1146	0.1546	3.06E-01
iron	**0.4079**	0.1344	2.90E-03	0.0807	0.1319	3.28E-01	bdl			0.1112	0.1493	2.77E-01	0.2426	0.1559	1.10E-01
$logK_{sw.Hg}$	0.2330	0.1324	5.37E-02	-0.0625	0.1324	7.17E-01	0.1167	0.1460	2.83E-01	0.2570	0.1501	6.21E-02	0.0938	0.1546	3.40E-01
$logK_{sw.MMHg}$	0.0739	0.1324	3.20E-01	0.1886	0.1387	1.20E-01	0.1083	0.1460	2.96E-01	0.1269	0.1501	2.49E-01	0.1647	0.1595	2.15E-01
magnesium	**0.4133**	0.1384	3.22E-03	**0.6592**	0.1360	4.22E-06	0.2281	0.1481	9.50E-02	**0.5068**	0.1491	7.50E-04	0.2969	0.1577	6.63E-02
manganese	**0.6512**	0.1351	7.35E-06	**0.3438**	0.1315	8.93E-03	bdl			**0.3822**	0.1517	1.08E-02	**0.3838**	0.1534	1.81E-02
$MMHg_{D}$	**0.3018**	0.1328	1.89E-02	**0.4750**	0.1387	7.71E-04	**0.4667**	0.1460	4.39E-03	**0.3591**	0.1501	1.46E-02	**0.3854**	0.1546	1.81E-02
$MMHg_{D}$:DOC	0.1818	0.1324	1.09E-01	**0.5159**	0.1387	3.08E-04	**0.3917**	0.1460	8.59E-03	0.1920	0.1501	1.34E-01	0.2083	0.1546	1.46E-01
$MMHg_{P.ngL}$	**0.3068**	0.1324	1.75E-02	0.2227	0.1387	8.03E-02	**0.4083**	0.1460	7.37E-03	0.2755	0.1501	5.11E-02	-0.0208	0.1546	6.15E-01
$MMHg_{P}$:TSS	0.1477	0.1324	1.64E-01	0.1477	0.1387	1.91E-01	0.0417	0.1460	4.19E-01	0.0433	0.1501	4.07E-01	0.0417	0.1546	4.50E-01
$MMHg_{T}$	**0.4091**	0.1324	2.75E-03	0.0057	0.1324	5.37E-01	-0.0667	0.1460	6.76E-01	0.0898	0.1501	3.14E-01	0.2292	0.1546	1.20E-01
nitrate	**0.5227**	0.1324	1.62E-04	**0.7045**	0.1324	6.92E-07	**0.5583**	0.1460	6.56E-04	**0.5913**	0.1501	2.04E-04	**0.5000**	0.1546	3.05E-03
Pct.C	0.1364	0.1324	1.78E-01	0.1932	0.1324	1.03E-01									
$PctHg_{D}$	**0.3920**	0.1324	3.32E-03	**0.4261**	0.1324	1.36E-03	**0.3750**	0.1460	1.13E-02	**0.5263**	0.1501	5.55E-04	-0.0521	0.1546	6.65E-01
$PctMMHg_{D}$	**0.3068**	0.1324	1.75E-02	**0.2841**	0.1387	3.12E-02	**0.4167**	0.1460	6.64E-03	**0.2941**	0.1501	4.17E-02	0.0833	0.1546	3.57E-01
phosphate							**0.3000**	0.1460	3.63E-02	bdl			0.1875	0.1546	1.73E-01
POC	**0.5909**	0.1324	3.33E-05	**0.3229**	0.1330	1.32E-02									
potassium	**0.5656**	0.1325	6.68E-05	**0.6353**	0.1327	4.81E-06	**0.4621**	0.1473	4.39E-03	0.0367	0.1555	4.17E-01	**0.5750**	0.1566	1.83E-03
SlopeRatio	0.0284	0.1324	4.48E-01	**0.4261**	0.1324	1.36E-03	**0.4000**	0.1460	7.69E-03	**0.7307**	0.1501	7.53E-06	**0.3542**	0.1546	2.93E-02
sodium	**0.6560**	0.1336	7.35E-06	**0.6133**	0.1348	1.20E-05	**0.4593**	0.1468	4.39E-03	**0.5560**	0.1491	3.83E-04	0.2064	0.1547	1.46E-01
SRP.P	**0.5227**	0.1324	1.62E-04	**0.6080**	0.1324	1.11E-05	**0.4000**	0.1460	7.69E-03	**0.2848**	0.1501	4.62E-02	0.1667	0.1546	2.08E-01
strontium	**0.2541**	0.1363	4.56E-02	**0.4726**	0.1344	5.84E-04	0.0752	0.1494	3.62E-01	**0.5686**	0.1546	4.27E-04	0.1058	0.1573	3.23E-01
sulfate	**0.5398**	0.1324	1.34E-04	**0.6648**	0.1324	2.07E-06	**0.5333**	0.1460	1.04E-03	**0.7492**	0.1501	6.00E-06	**0.4479**	0.1546	6.84E-03
$SUVA_{254}$	0.2330	0.1324	5.37E-02	0.0455	0.1324	4.30E-01	0.0583	0.1460	3.94E-01	0.1548	0.1501	1.95E-01	**0.4896**	0.1546	3.42E-03
TSS	**0.4987**	0.1337	3.56E-04	0.1035	0.1319	2.79E-01	**0.4250**	0.1460	6.64E-03	0.2570	0.1501	6.21E-02	0.2512	0.1538	1.08E-01
uranium	**0.2672**	0.1322	3.41E-02	**0.4953**	0.1331	3.08E-04	**0.2913**	0.1464	3.88E-02	**0.6319**	0.1516	1.23E-04	**0.5302**	0.1516	1.88E-03

Table S.5 (cont.)

	Su2018, EFK 5.4					
	Surface water			Pore water		
Variable	ξ	sd	pval	ξ	sd	pval
Hg_D	0.0917	0.1460	2.65E-01	0.1734	0.1501	2.48E-01
$Hg_{P.ngL}$	0.2250	0.1460	1.02E-01			
Hg_T	0.3000	0.1460	5.98E-02			
$MMHg_D$	0.3417	0.1460	5.78E-02	-0.1083	0.1460	7.71E-01
$MMHg_{P.ngL}$	0.2000	0.1460	1.02E-01			
$MMHg_T$	0.2083	0.1460	1.02E-01			

Sonde data															
Campaign	Su2013			W2014			Su2015								
Site	EFK 5.4			EFK 5.4			EFK 5.4			EFK 16.2			EFK 23.4		
Variable	ξ	sd	pval	ξ	sd	pval	ξ	sd	pval	ξ	sd	pval	ξ	sd	pval
Temp.C	**0.9289**	0.0577	0.00E+00	**0.9513**	0.0576	0.00E+00	**0.9294**	0.0578	0.00E+00	**0.9315**	0.0577	0.00E+00	**0.9265**	0.0577	0.00E+00
SpecCond	**0.8792**	0.0594	0.00E+00	**0.9550**	0.0600	0.00E+00	**0.9099**	0.0579	0.00E+00	**0.9556**	0.0578	0.00E+00	**0.9245**	0.0578	0.00E+00
pH	**0.9056**	0.0583	0.00E+00	**0.9168**	0.0568	0.00E+00	**0.8733**	0.0589	0.00E+00	**0.8752**	0.0584	0.00E+00	**0.9043**	0.0586	0.00E+00
ODO.PctSat	**0.9182**	0.0576	0.00E+00	**0.9329**	0.0576	0.00E+00	**0.9330**	0.0579	0.00E+00	**0.8954**	0.0579	0.00E+00	**0.9189**	0.0575	0.00E+00
DO.mgL	**0.9262**	0.0577	0.00E+00	**0.9205**	0.0575	0.00E+00	**0.9339**	0.0578	0.00E+00	**0.8988**	0.0578	0.00E+00	**0.9268**	0.0577	0.00E+00
Turbidity	**0.5760**	0.0574	0.00E+00	**0.1847**	0.0578	7.04E-04	**0.7026**	0.0580	0.00E+00	**0.5201**	0.0577	0.00E+00			
FDOM	**0.7907**	0.0577	0.00E+00	**0.9277**	0.0575	0.00E+00									
Q.cms	**0.8887**	0.0575	0.00E+00	**0.8710**	0.0575	0.00E+00	**0.9238**	0.0577	0.00E+00	**0.6714**	0.0577	0.00E+00	**0.7999**	0.0583	0.00E+00

Table S.6. Spearman rank correlation coefficients (p-value) between $Hg_{P.ngL}$, $MMHg_{P.ngL}$, and TSS. p-values were corrected for multiple comparisons using the method of Benjamini and Hochberg [5]. Values in bold typeface have p-values ≤ 0.05

Event	Site	$Hg_{P.ngL}$	$MMHg_{P.ngL}$
Su2013	EFK 5.4	**0.758** (2.79e-5)	**0.442** (0.0347)
W2014	EFK 5.4	**0.583** (3.52e-3)	0.203 (0.378)
Su2015	EFK 5.4	**0.739** (3.04e-4)	**0.640** (3.14e-3)
	EFK 16.2	**0.643** (4.00e-3)	**0.719** (7.67e-4)
	EFK 23.4	-0.0944 (0.719)	0.0368 (0.889)

Table S.7. Spearman rank correlation coefficients (p-value) between Hg_D, $MMHg_D$, and DOC. p-values were corrected for multiple comparisons using the method of Benjamini and Hochberg [5]. Values in bold typeface have p-values ≤ 0.05

Event	Site	Hg_D	$MMHg_D$
Su2013	EFK 5.4	**0.58** (4.69e-3)	0.422 (0.0503)
W2014	EFK 5.4	-0.22 (0.308)	0.0435 (0.851)
Su2015	EFK 5.4	0.05 (0.839)	0.425 (0.0699)
	EFK 16.2	**-0.719** (7.67e-3)	0.119 (0.639)
	EFK 23.4	**0.867** (6.67e-6)	**0.59** (0.0127)

Table S.8. Spearman rank correlation coefficients (p-value) between DOC, $SUVA_{254}$, Hg_D, $MMHg_D$, and FDOM. p-values were corrected for multiple comparisons using the method of Benjamini and Hochberg [5]. Values in bold typeface have p-values ≤ 0.05

Event	Site	DOC	$SUVA_{254}$	Hg_D	$MMHg_D$
Su2013	EFK 5.4	0.187 (0.81)	0.054 (0.81)	0.131 (0.81)	-0.0862 (0.81)
		0.0812 (0.757)[a]	-0.236 (0.69)[a]	0.142 (0.757)[a, b]	-0.329 (0.69)[a]
W2014	EFK 5.4	**0.489 (0.042)**	0.124 (0.574)	**-0.821 (6.35e-6)**	**-0.66 (2.29e-3)**

[a] potential FDOM outliers excluded
[b] potential FDOM and Hg_D outliers excluded

Table S.9. Constituent loading and time-weighted mean concentration (TWMC) for each sampling event and location[a]

			Su2013	W2014		Su2015		Su2018
Parameter	**Metric**	**Units**	**EFK 5.4**	**EFK 5.4**	**EFK 5.4**	**EFK 16.2**	**EFK 23.4**	**EFK 5.4**
aluminum	Load	kg	1.069	1.877	11.98	3.855	0.3108	—
	TWMC	$\mu g \cdot L^{-1}$	8.432	9.550	139.8	82.93	28.82	—
ammonium.N	Load	kg	1.619	—	1.809	1.103	0.3599	—
	TWMC	$\mu g\text{-}N \cdot L^{-1}$	12.74	—	22.01	23.50	32.90	—
barium	Load	kg	5.211	6.625	6.164	2.772	0.6775	—
	TWMC	$\mu g \cdot L^{-1}$	41.13	33.66	71.84	59.58	62.27	—
bromide	Load	kg	—	—	2.171	6.055	3.928	—
	TWMC	$mg \cdot L^{-1}$	—	—	0.0314	0.1365	0.3597	—
calcium	Load	kg	6356	9001	3910	2306	537.2	—
	TWMC	$mg \cdot L^{-1}$	50.16	45.74	47.53	49.87	49.33	—
chloride	Load	kg	1819	2685	1683	728	263.0	—
	TWMC	$mg \cdot L^{-1}$	14.36	13.67	20.44	15.79	24.13	—
DOC	Load	kg	252.5	285.0	187.4	68.96	13.99	—
	TWMC	$mg \cdot L^{-1}$	1.992	1.450	2.269	1.482	1.283	—
Hg_D	Load	g	1.466	1.864	1.557	1.106	0.7696	3.218
	TWMC	$ng \cdot L^{-1}$	11.57	9.468	19.0	23.9	70.6	25.6
$Hg_{P.ngL}$	Load	g	10.41	12.46	3.986	2.881	0.576	18.35
	TWMC	$ng \cdot L^{-1}$	82.31	63.19	48.94	64.19	52.86	146.0
Hg_T	Load	g	11.88	14.32	5.543	3.987	1.346	21.57
	TWMC	$ng \cdot L^{-1}$	93.88	72.66	67.89	88.12	123.4	171.6
iron	Load	kg	9.949	50.24	bdl[b]	5.082	0.8623	—
	TWMC	$\mu g \cdot L^{-1}$	78.54	262.1		109.2	79.22	—
magnesium	Load	kg	1328	1786	900	538	132.7	—
	TWMC	$mg \cdot L^{-1}$	10.49	9.082	10.94	11.66	12.18	—
manganese	Load	g	977.7	3948	bdl[b]	429.0	92.65	—
	TWMC	$\mu g \cdot L^{-1}$	7.730	20.45		9.115	8.527	—
$MeHg_D$	Load	mg	31.62	17.63	20.60	7.678	0.8707	55.92
	TWMC	$ng \cdot L^{-1}$	0.2493	0.0897	0.2504	0.1654	0.0799	0.4456
$MeHg_{P.ngL}$	Load	mg	13.23	4.336	5.836	4.826	0.2976	15.79
	TWMC	$ng \cdot L^{-1}$	0.1044	0.0221	0.0714	0.1071	0.0274	0.1251
$MeHg_T$	Load	mg	44.85	23.48	26.44	12.50	1.168	71.71
	TWMC	$ng \cdot L^{-1}$	0.3537	0.1191	0.3218	0.2725	0.1073	0.5707
nitrate	Load	kg	1729	1936	1990	252.9	138.1	—
	TWMC	$mg \cdot L^{-1}$	13.65	9.878	24.06	5.494	12.68	—
phosphate	Load	kg	—	—	275.9	bdl[b]	4.504	—
	TWMC	$mg \cdot L^{-1}$	—	—	3.322		0.4118	—
POC	Load	kg	37.02	55.00	—	—	—	—
	TWMC	$mg \cdot L^{-1}$	0.2912	0.2798	—	—	—	—
potassium	Load	kg	372.0	426.3	327.2	93.58	22.14	—
	TWMC	$mg \cdot L^{-1}$	2.938	2.169	3.974	2.022	2.031	—
sodium	Load	kg	1319	1760	1172	424.9	155.6	—
	TWMC	$mg \cdot L^{-1}$	10.42	8.956	14.21	9.232	14.28	—
SRP.P	Load	kg	48.49	8.533	63.06	1.888	0.8416	—
	TWMC	$\mu g\text{-}P \cdot L^{-1}$	382.9	43.64	762.8	40.30	77.13	—
strontium	Load	kg	12.88	17.24	9.327	6.080	1.539	—
	TWMC	$\mu g \cdot L^{-1}$	101.7	87.64	113.3	131.5	141.3	—
sulfate	Load	kg	2883	3749	2194	1442	389.3	—
	TWMC	$mg \cdot L^{-1}$	22.77	19.07	26.68	31.24	35.73	—
TSS	Load	kg	733.4	870.8	298.2	197.2	27.11	—
	TWMC	$mg \cdot L^{-1}$	5.774	4.420	3.612	4.321	2.486	—
uranium	Load	g	788.4	745.1	243.9	206.5	87.66	—
	TWMC	$\mu g \cdot L^{-1}$	6.222	3.782	2.964	4.490	8.048	—

[a] Loads for Su2018 can be multiplied by 0.625 to correct for the longer sampling time to facilitate comparison to the other sampling events

[b] most results below method reporting limit

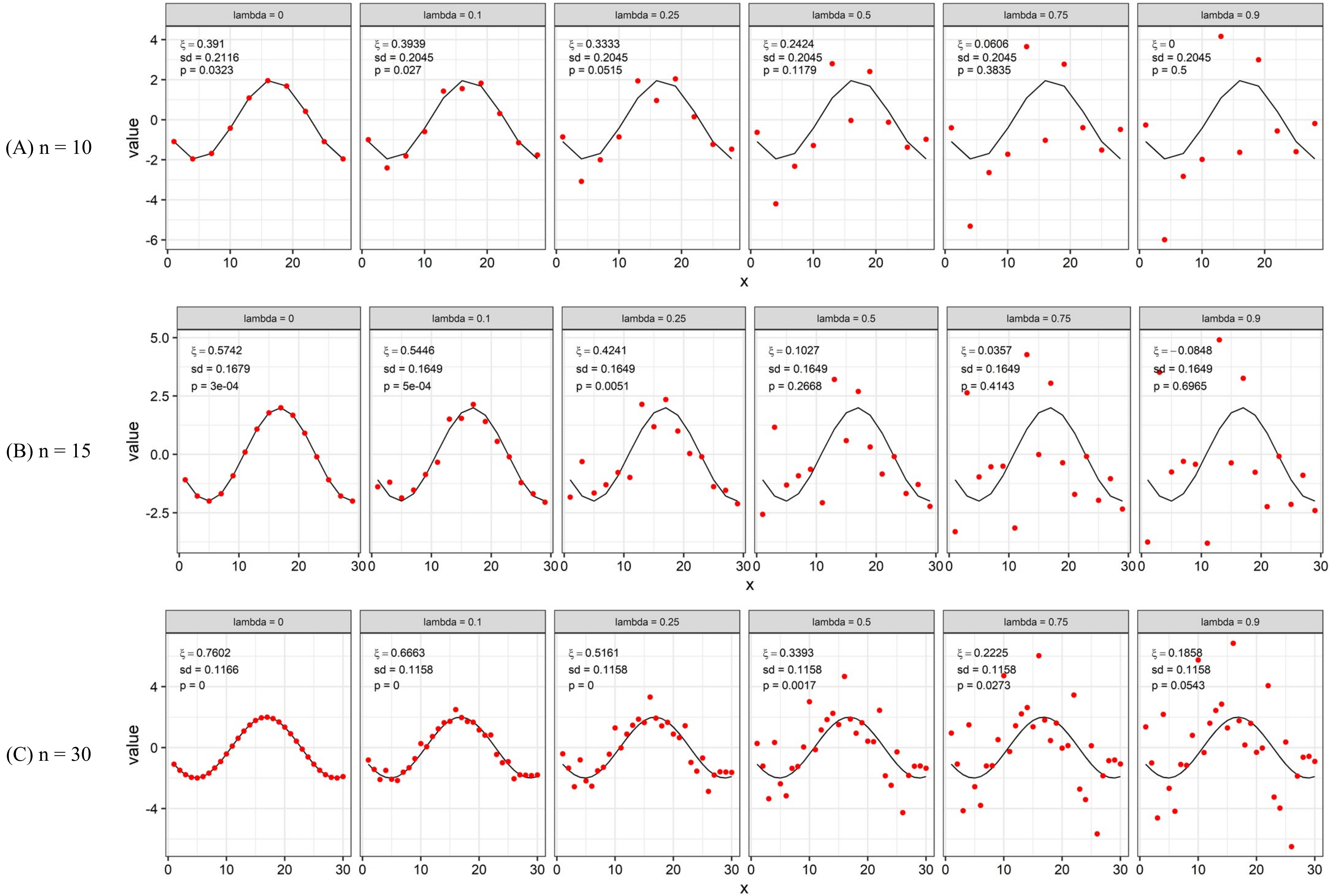

Figure S.1. Behavior of the dependence measure (ξ) at different noise levels (lambda = 0 is the noise-free data) and number of data points (A) n = 10, (B) n = 15, (C) n = 30. Black line shows the noise-free data in each plot. sd = standard deviation of ξ; p = p-value. Note that n = 16 is the minimum number of observations in the data sets in the paper.

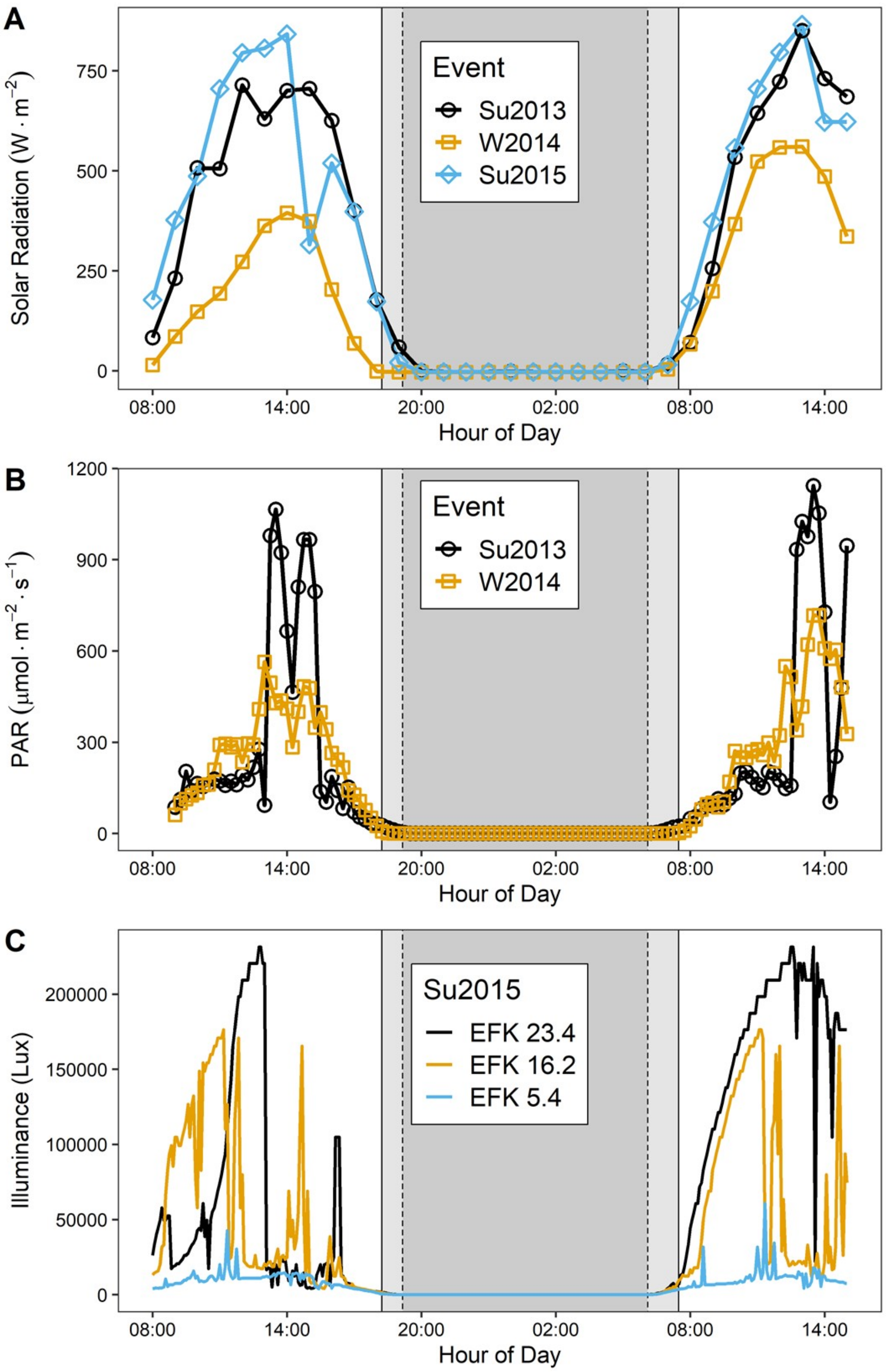

Figure S.2. (A) Solar radiation measured at a nearby meteorological tower for each sampling campaign, (B) photosynthetically active radiation measured 30 cm above the water surface at EFK 5.4 for the Su2013 and W2014 campaigns, and (C) total light intensity measured creek-side at each location for the Su2015 campaign.

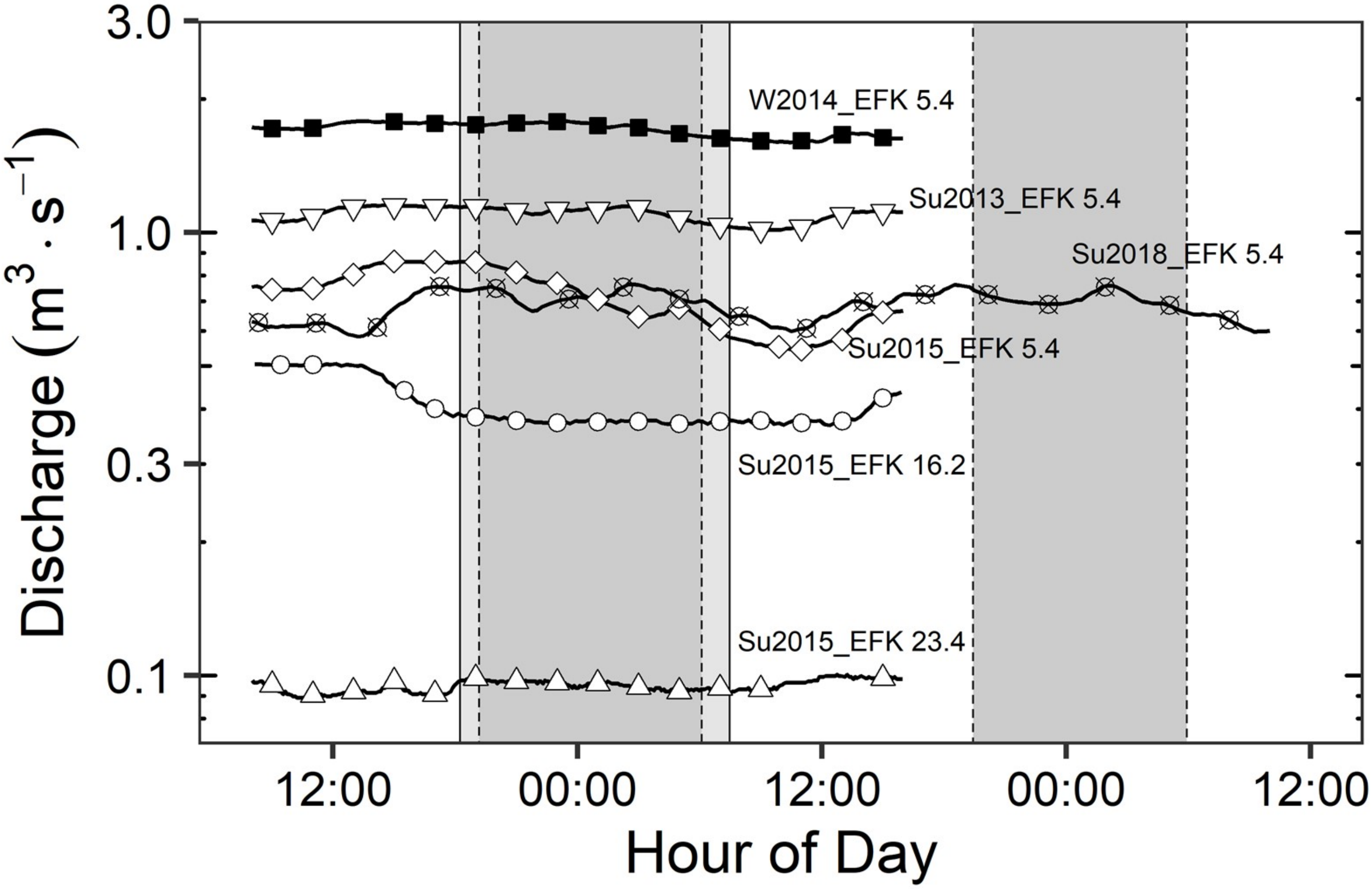

Figure S.3. Creek discharge for each sampling campaign and location. Symbols indicate when samples were collected. Shaded portions indicate the period from sunset to sunrise.

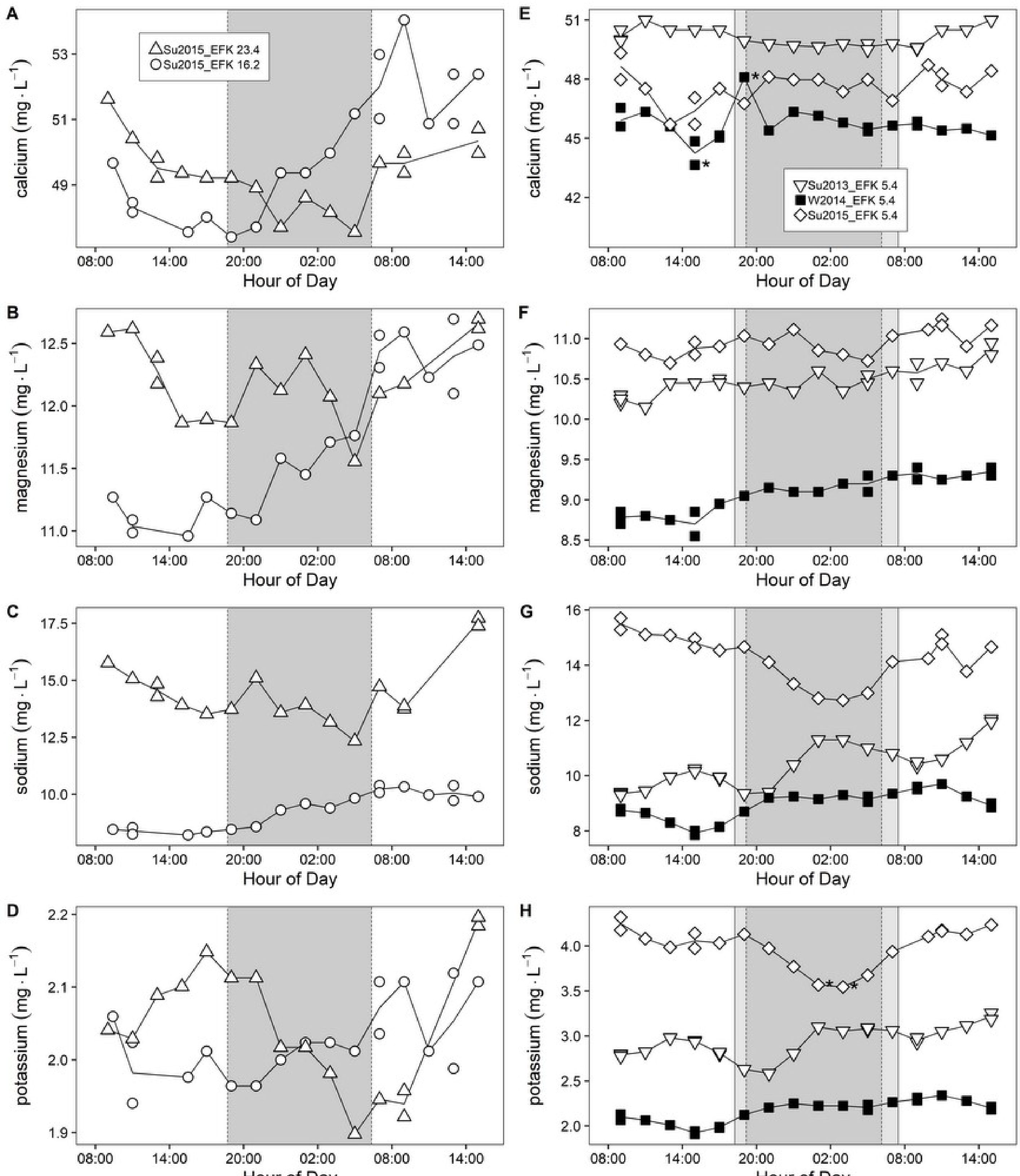

Figure S.4. Calcium, magnesium, sodium, and potassium concentrations for the diel sampling campaigns. (A)-(D) Su2015 campaign at EFK 23.4 and EFK 16.2, (E)-(H) Su2013, W2014, and Su2015 campaigns at EFK 5.4. Shaded portions indicate the period from sunset to sunrise. Asterisks to the right of symbols indicate potential outliers.

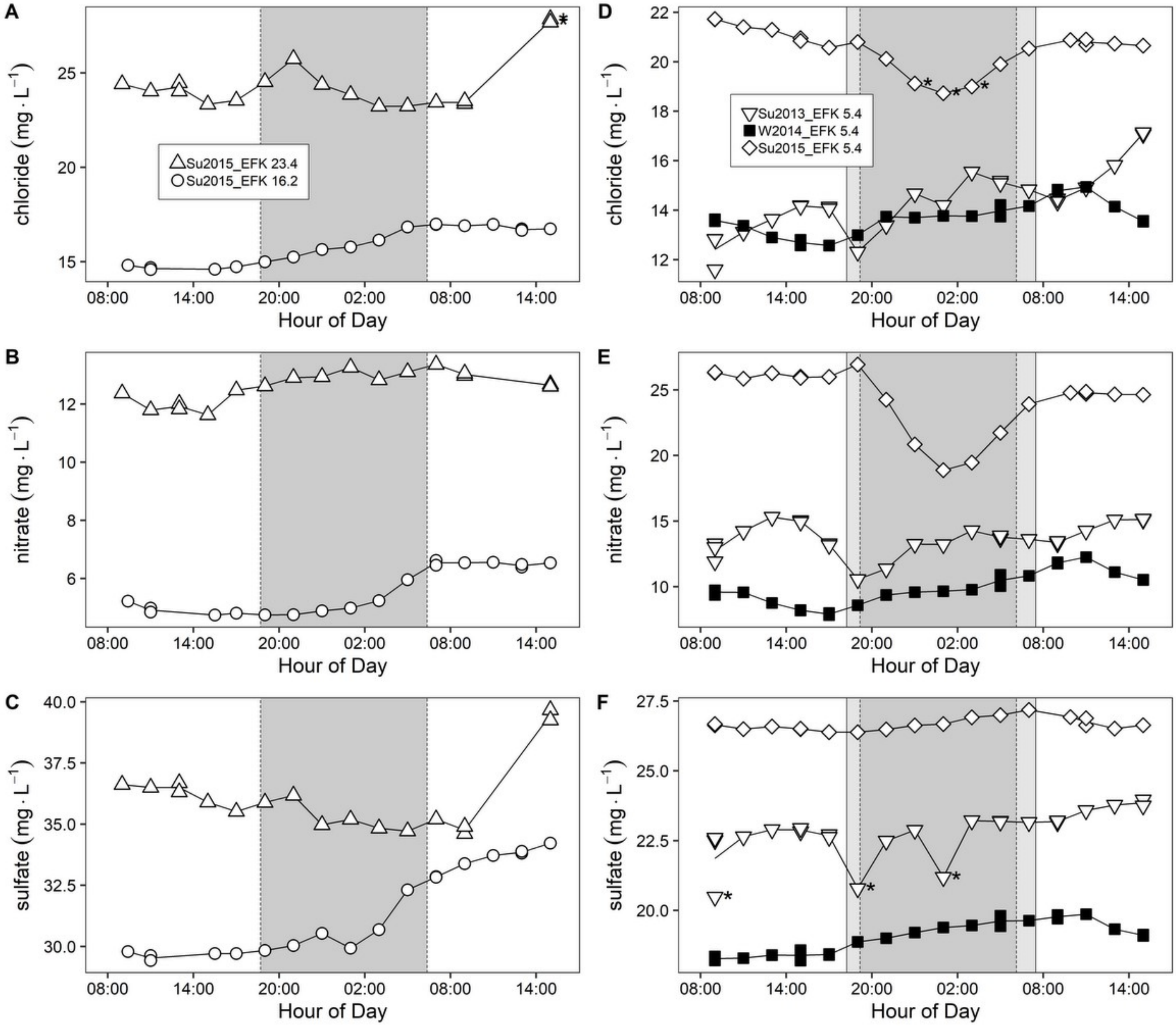

Figure S.5. Chloride, nitrate, and sulfate concentrations for the diel sampling campaigns. (A)-(C) Su2015 campaign at EFK 23.4 and EFK 16.2, (D)-(F) Su2013, W2014, and Su2015 campaigns at EFK 5.4. Shaded portions indicate the period from sunset to sunrise. Asterisks to the right of symbols indicate potential outliers.

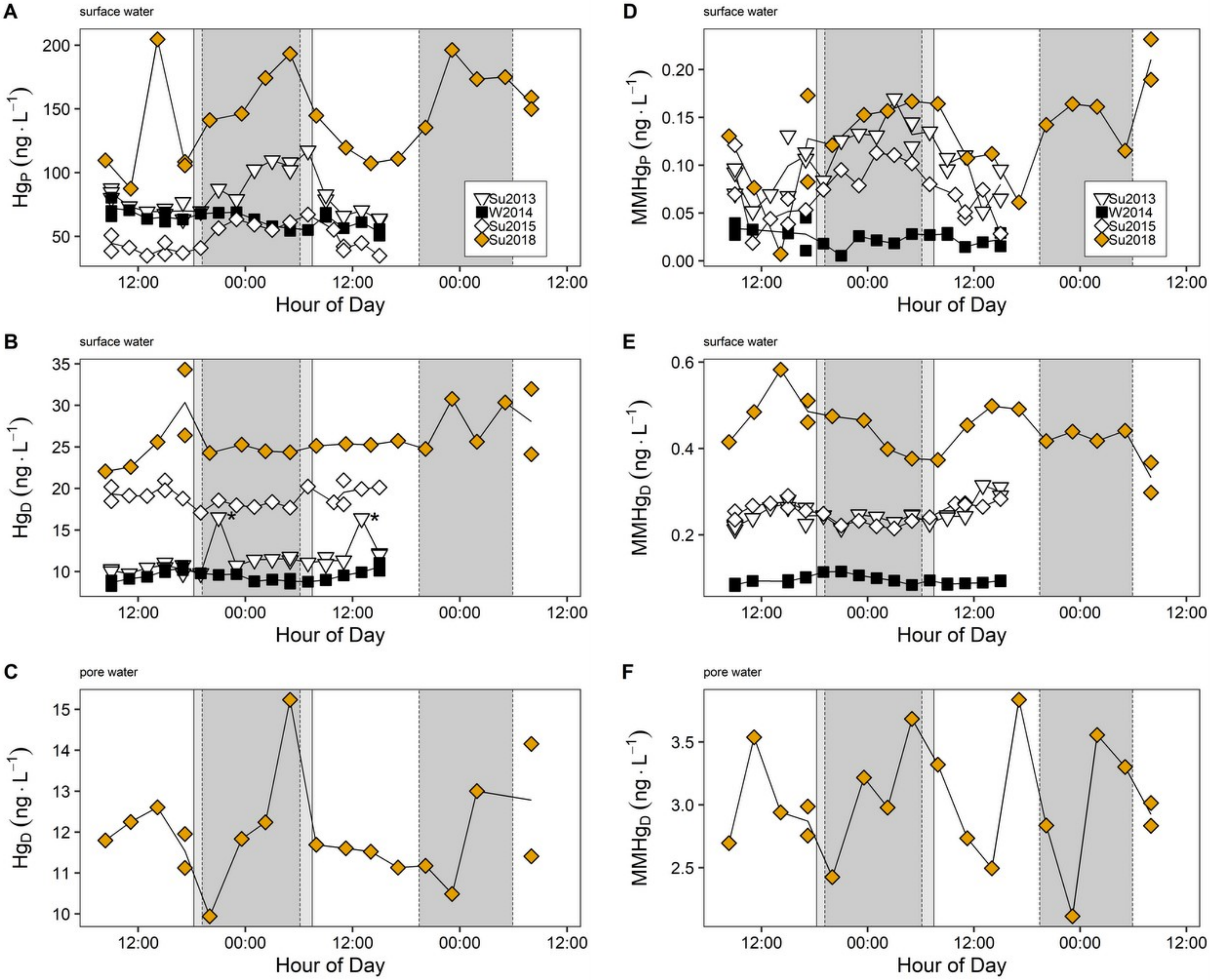

Figure S.6. Particulate and dissolved total Hg (A – C) and MMHg (D – F) in surface water(A, B, D, E) and interstitial pore water (C, F) at EFK 5.4 including data from the Su2018 48-hour sampling campaign. Asterisks to the right of symbols indicate potential outliers.

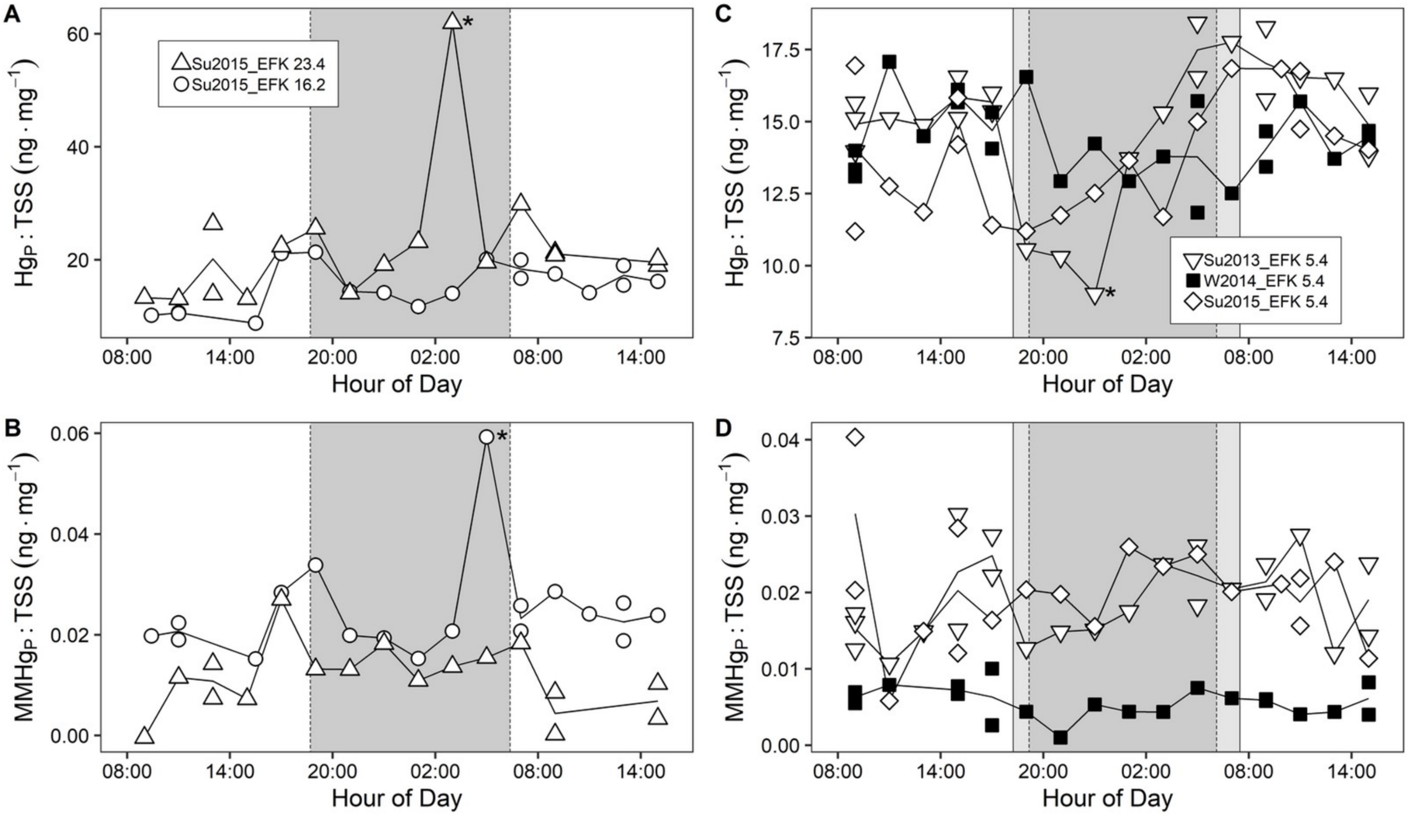

Figure S.7 Particle-specific Hg and MMHg concentration (milligram per kilogram dry weight TSS) for each diel sampling campaign. (A)-(B) Su2015 campaign at EFK 23.4 and EFK 16.2, (C)-(D) Su2013, W2014, and Su2015 campaigns at EFK 5.4. Shaded portions indicate the period from sunset to sunrise. Asterisks to the right of symbols indicate potential outliers.

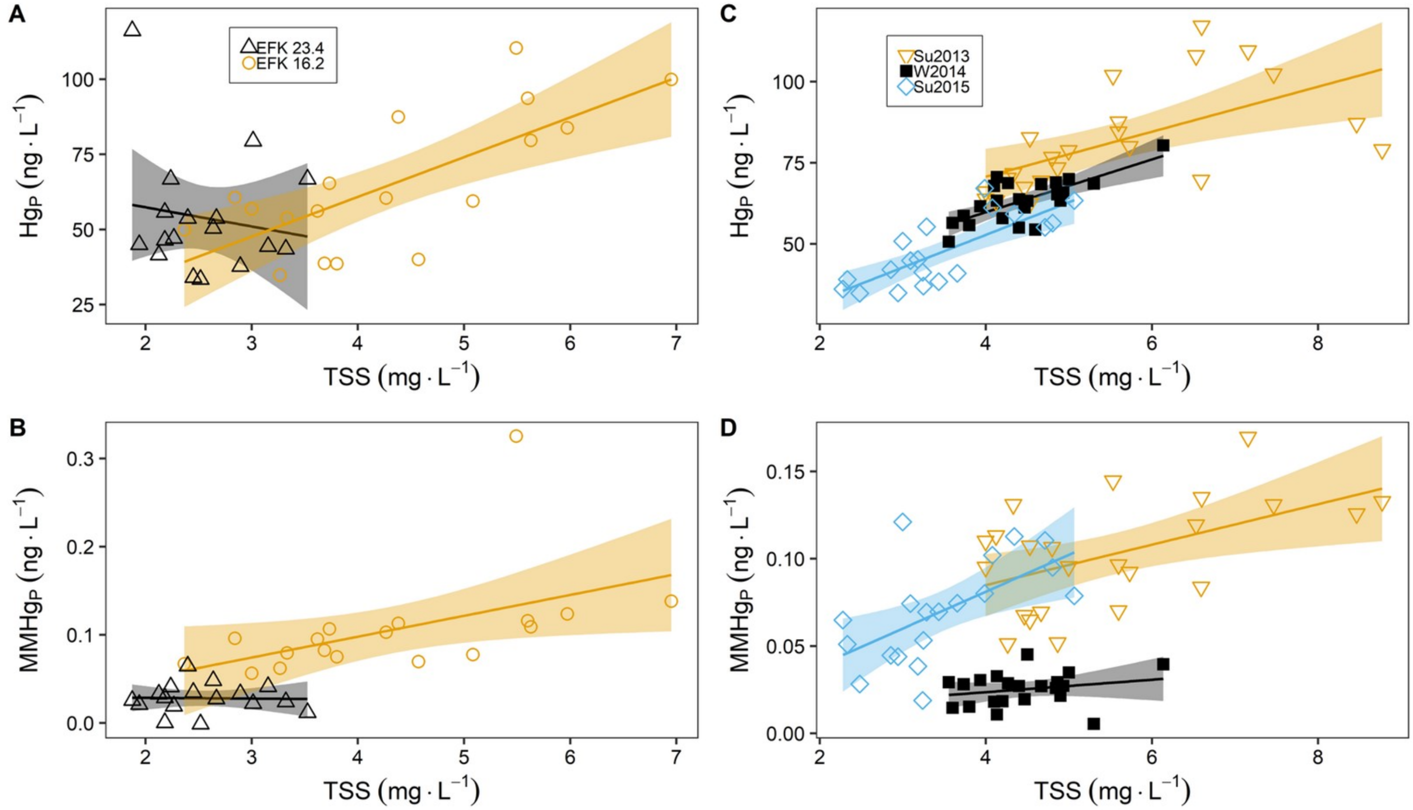

Figure S.8. Particulate Hg (upper row) and MMHg (lower row) versus TSS for each diel sampling campaign. (A)-(B) Su2015 campaign at EFK 23.4 and EFK 16.2, (C)-(D) Su2013, W2014, and Su2015 campaigns at EFK 5.4. Regression lines and their 95% confidence regions are shown.

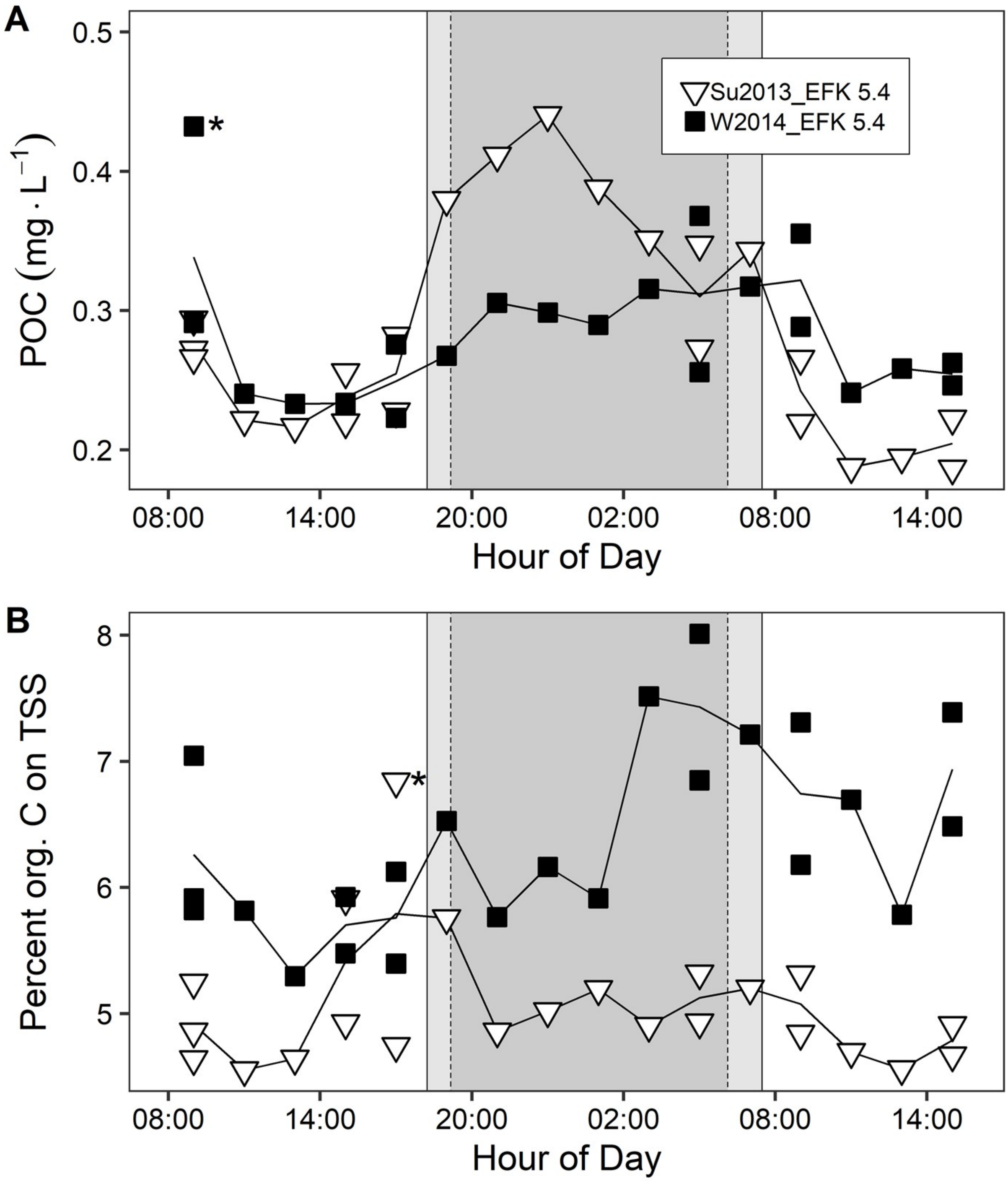

Figure S.9. (A) Particulate organic carbon and (B) percent organic carbon on TSS (dry weight basis) at EFK 5.4 during the Su2013 and W2014 sampling campaigns. Shaded portions indicate the period from sunset to sunrise. Asterisks to the right of symbols indicate potential outliers.

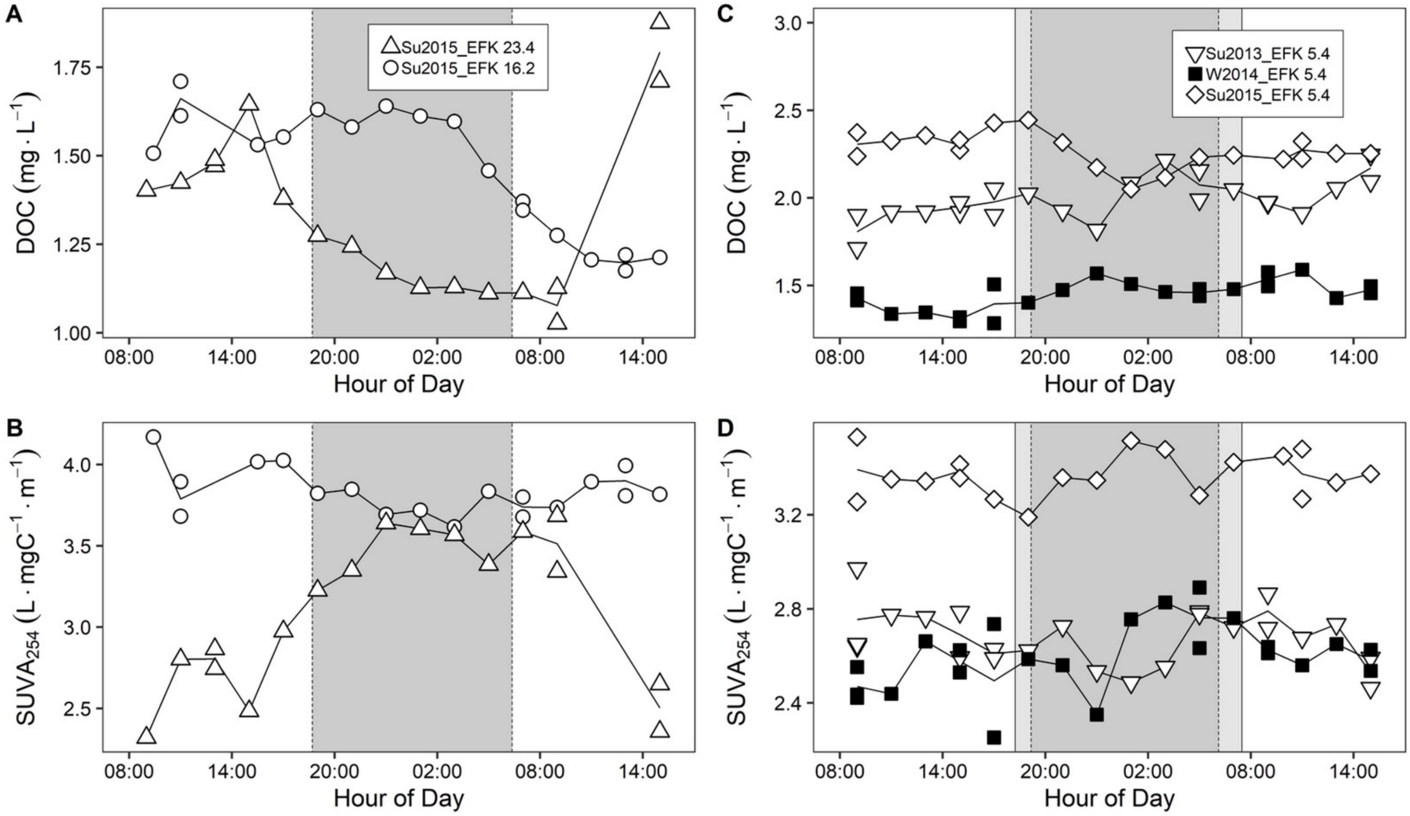

Figure S.10 DOC concentration and $SUVA_{254}$ for each diel sampling campaign. (A)-(B) Su2015 campaign at EFK 23.4 and EFK 16.2, (C)-(D) Su2013, W2014, and Su2015 campaigns at EFK 5.4. Shaded portions indicate the period from sunset to sunrise.

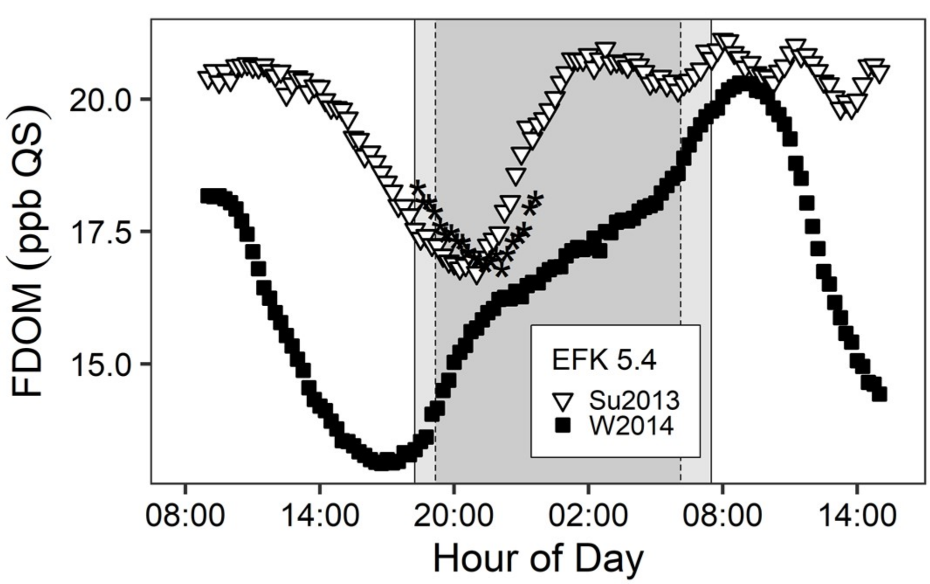

Figure S.11. Fluorescent dissolved organic matter at EFK 5.4 for the Su2013 and W2014 sampling campaigns. Shaded portions indicate the period from sunset to sunrise. Asterisks to the right of symbols indicate potential outliers.

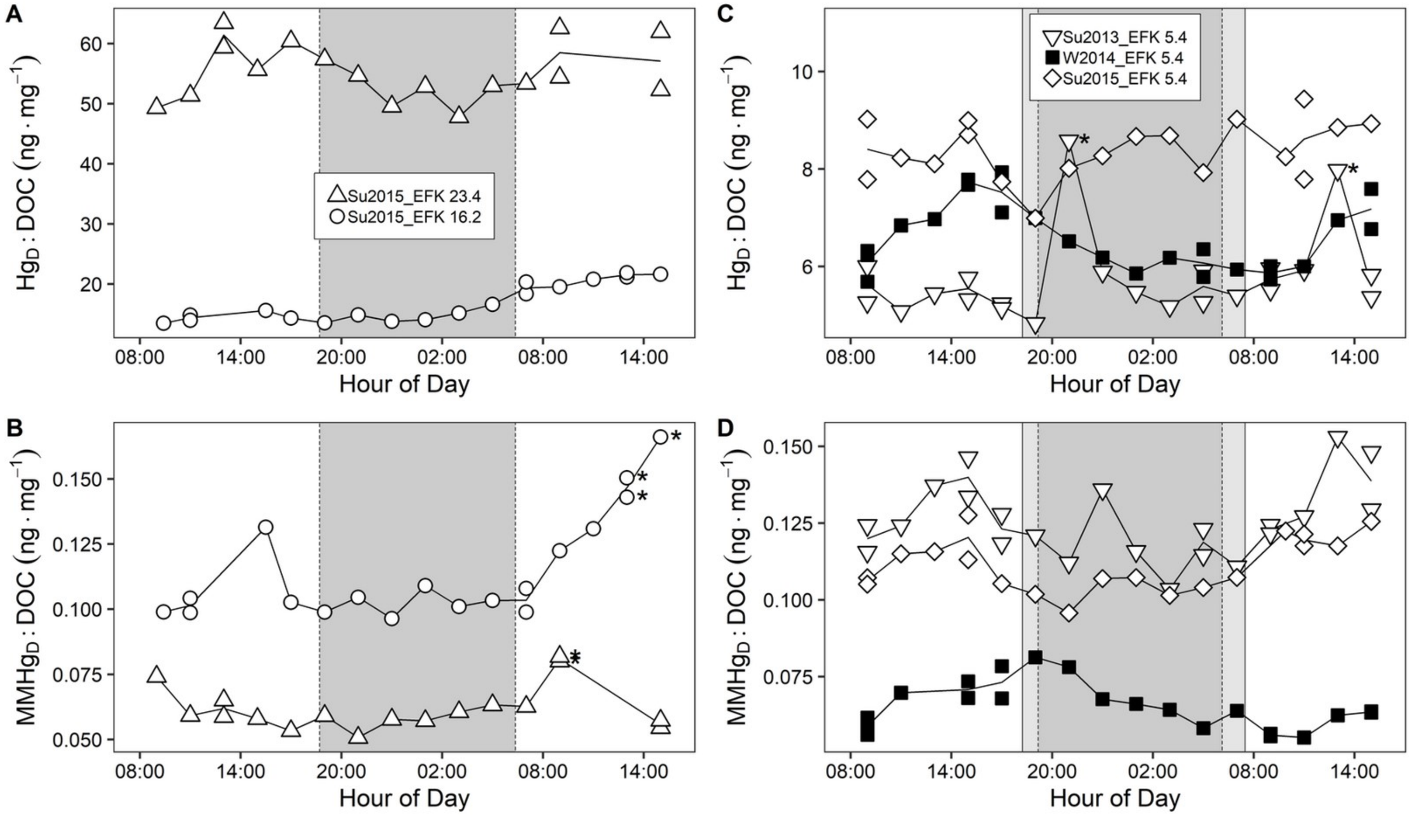

Figure S.12 Ratio of dissolved total Hg and MMHg to DOC for each diel sampling campaign. (A)-(B) Su2015 campaign at EFK 23.4 and EFK 16.2, (C)-(D) Su2013, W2014, and Su2015 campaigns at EFK 5.4. Shaded portions indicate the period from sunset to sunrise. Asterisks to the right of symbols indicate potential outliers.

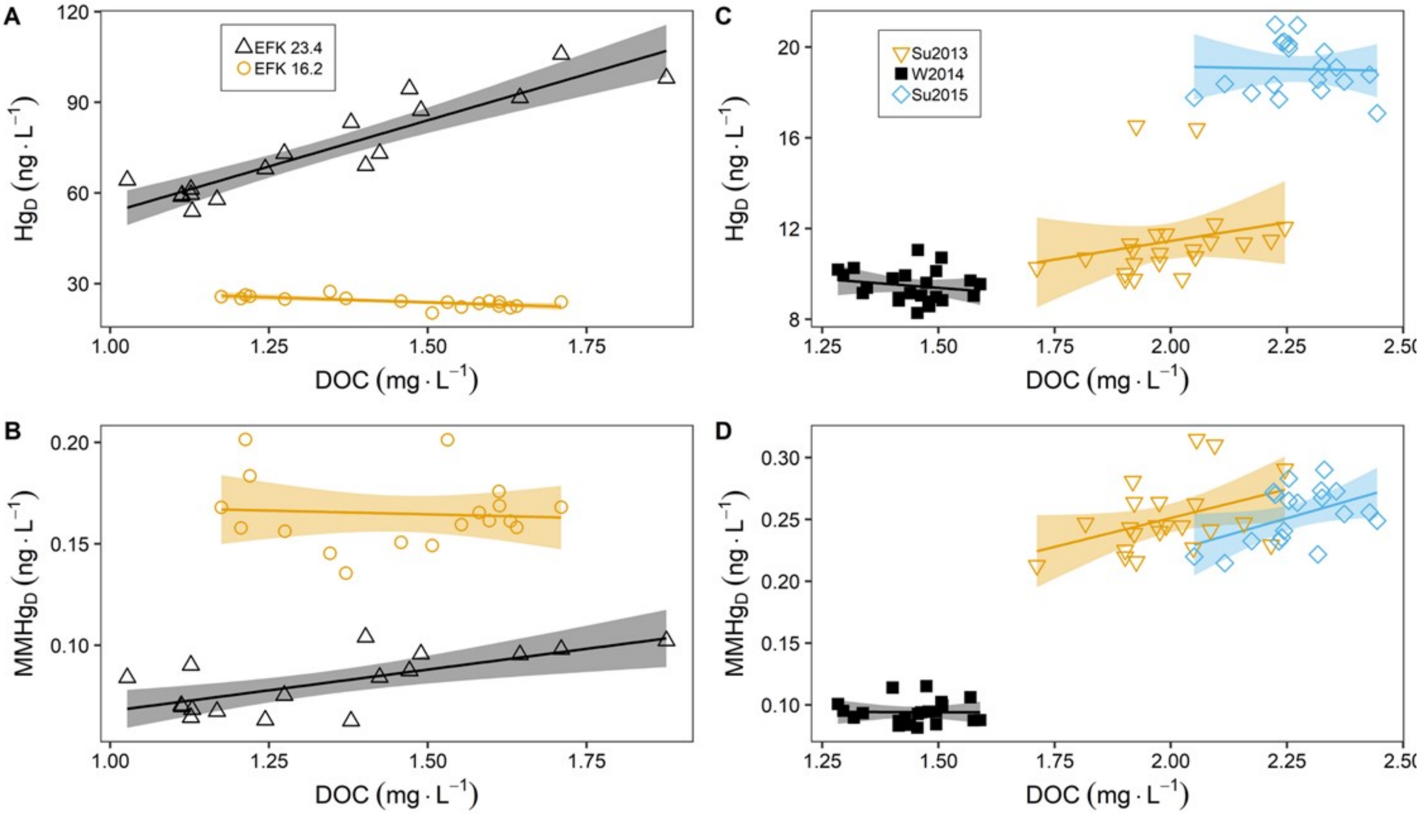

Figure S.13 Dissolved total Hg and MMHg concentration versus DOC for each sampling campaign. (A)-(B) Su2015 campaign at EFK 23.4 and EFK 16.2, (C)-(D) Su2013, W2014, and Su2015 campaigns at EFK 5.4.

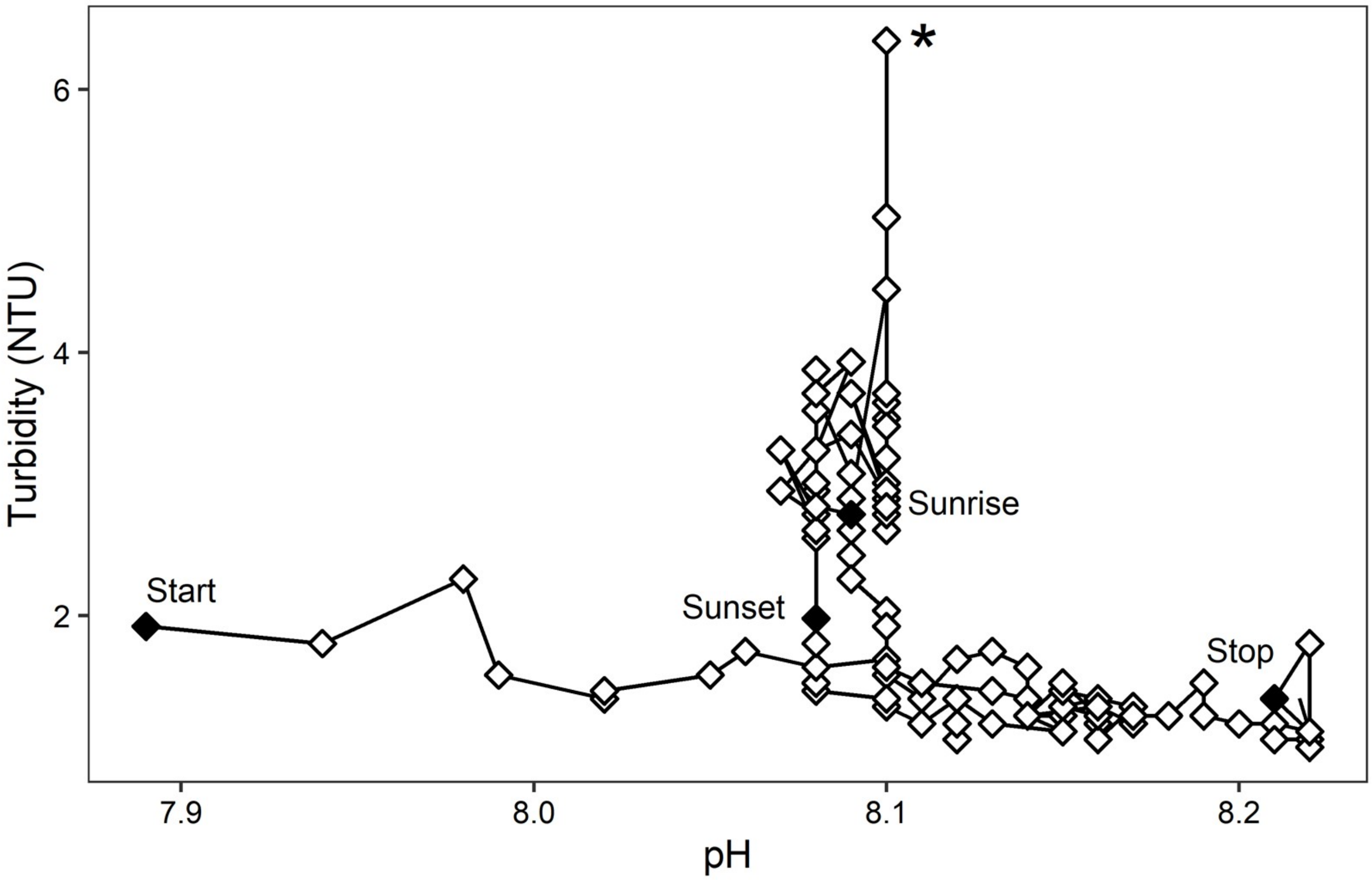

Figure S.14. Turbidity versus pH hysteresis curve for EFK 5.4 during the Su2015 campaign. The trace proceeds from left to right. From the start of sampling turbidity remained constant while pH increased then decreased. After sunset, turbidity increased while pH did not change. Shortly after sunrise, turbidity gradually decreased while pH increased. Asterisk to the right of symbol indicates potential outlier.

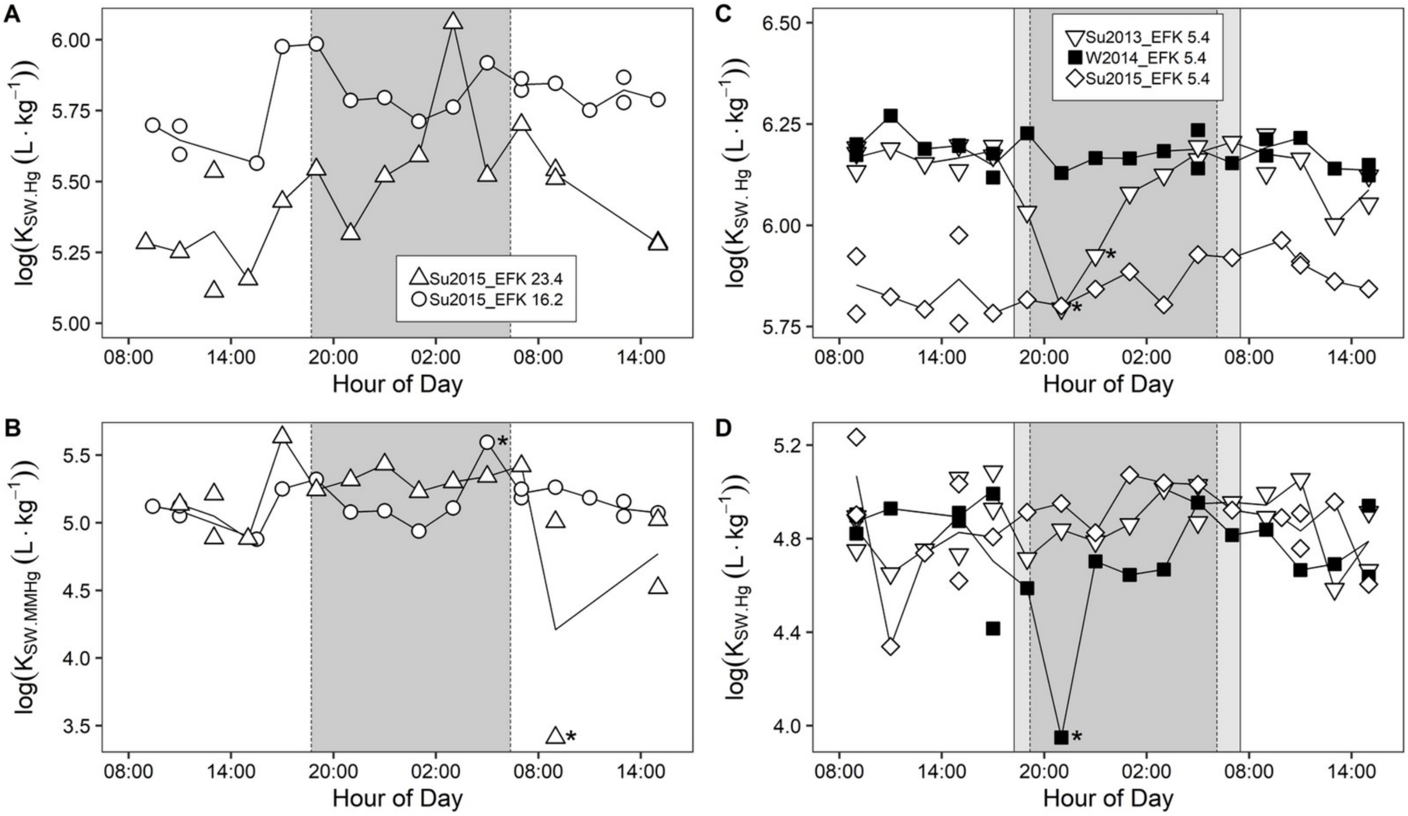

Figure S.15 Solid-water partitioning coefficients for Hg and MMHg for each diel sampling campaign. (A)-(B) Su2015 campaign at EFK 23.4 and EFK 16.2, (C)-(D) Su2013, W2014, and Su2015 campaigns at EFK 5.4. Shaded portions indicate the period from sunset to sunrise. Asterisks to the right of symbols indicate potential outliers.

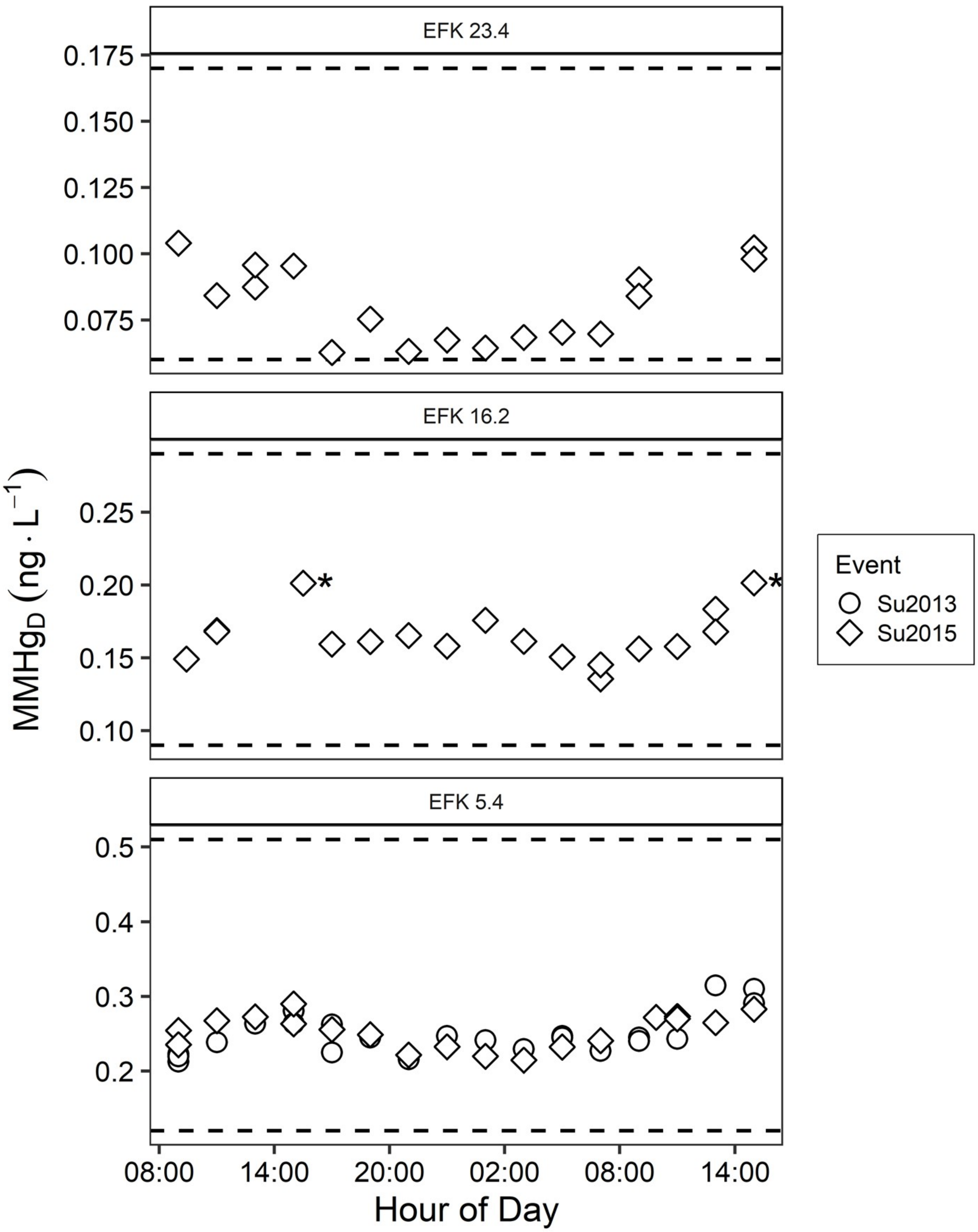

Figure S.16. Diel variability in summer $MMHg_D$ concentration at each site against a backdrop of the annual variability from monthly samples collected at a consistent time of day at baseflow over the period August 2013 through September 2015. Horizontal dashed lines represent the range of values at each site over that period. Asterisks to the right of symbols indicate potential outliers.

7. REFERENCES

1. L. Oppenheimer, T. P. Capizzi, R. M. Weppelman and H. Mehta, Determination of the lowest limit of reliable assay measurement, *Anal. Chem*, 1983, **55**, 638-643.
2. NIST, http://www.itl.nist.gov/div898/handbook/eda/section3/eda35h.htm, (accessed 30 May 2017).
3. R. E. Shiffler, Maximum z-scores and outliers, *American Statistician*, 1988, **42**, 79-80.
4. S. Chatterjee, A New Coefficient of Correlation, *Journal of the American Statistical Association*, 2021, **116**, 2009-2022.
5. Y. Benjamini and Y. Hochberg, Controlling the False Discovery Rate: A Practical and Powerful Approach to Multiple Testing, *Journal of the Royal Statistical Society: Series B (Methodological)*, 1995, **57**, 289-300.